Kinetic and Structural Factors Governing Chiral Recognition in Cobalt(III) Chiroporphyrin−Amino Alcohol Complexes

Jean-Pierre Simonato, Jacques Pécaut, and Jean-Claude Marchon*

Laboratoire de Chimie de Coordination, SCIB Département de Recherche Fondamentale sur la Matière Condensée, CEA-Grenoble, 38054 Grenoble, France

Received February 26, 1998

Recently we reported on the binding of optically active alcohol and amine axial ligands to ruthenium(II) and cobalt(III) α,*β*,α,*β*-tetramethylchiroporphyrins,[1−3] two chiral metallohosts derived from enantiopure (1*R*)-*cis*-hemicaronaldehyde (biocartol).[4] On each face of the TMCP macrocycle, along a $C_{meso}-C_{meso}$ axis, the chiral *meso* substituents define a C_2-symmetric groove of ca. 3−4 Å width which can accommodate an axial guest. The crystal structures of the alcohol and amine adducts revealed similar multipoint interaction between guest and metallohost, using convergent *σ*-donation to the metal center, and O(N)−H···O and C−H···O hydrogen bonding to the *meso* substituents of the chiroporphyrin. Yet enantiomer recognition ((*R*)/(*S*) ≈ 2 at −50 °C) was observed only for the chiral alcohols bound to the ruthenium(II) metalloreceptor Ru(CO)(TMCP).[2] We found that the binding of chiral amines to chlorocobalt(III) tetramethylchiroporphyrin (CoCl(EtOH)(TMCP), **1**) is irreversible, and the lack of enantioselection in that case was attributed to the kinetic control of bis-amine complex formation.[3] We now report that under similar conditions chiral recognition of *β*-amino alcohols by the cobalt(III) complex **1** can be observed. This host−guest system slowly reaches equilibrium over a period of 20−80 h. The crystal structures of the adducts of (*R*)- and (*S*)-prolinol with **1** provide a rationale for the selection of the (*R*) enantiomer, which is observed in these systems.[5]

Addition to **1** in $CDCl_3$ solution of 2 equiv of one of the enantiopure *β*-amino alcohols **2**−**7** led to distinct, ring-current-shifted ^{1}H NMR signatures in the range +1.3 to −6.5 ppm for the coordinated (*R*) and (*S*) enantiomers. The proposed signal

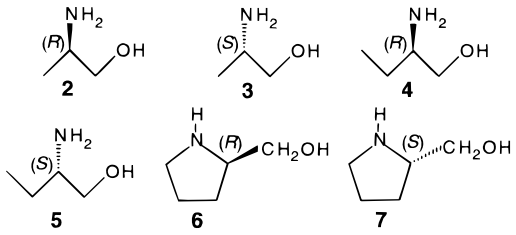

attributions have been obtained by 2D ^{1}H NMR experiments, and they are collected in Table S1 (Supporting Information). The large chemical shift difference ($\Delta\delta \geq 1.2$ ppm; 240 Hz at 200 MHz) observed for the two amine protons N−H_d and N−H_e of **2**−**5** suggests a downfield shift by N−H···O hydrogen bonding of H_d, which has been confirmed in the crystal structures of the adducts of **3** and **5** (*vide infra*). The observed shift differences $|\Delta\delta_{RS}|$ between coordinated enantiomers (0.1−0.3 ppm; 20−60 Hz at 200 MHz) are as large as those obtained with the best chiral shift reagents for amines,[6] allowing the relative concentrations of the (*R*) and (*S*) ligands to be readily determined.[7,8]

Upon addition of excess racemic *β*-amino alcohol (ca. 3 equiv each of **2**+**3**, or **4**+**5**, or **6**+**7**) to **1** in $CDCl_3$ solution, the resonances of the two cobalt-bound enantiomers initially appear in a 1:1 intensity ratio. However, monitoring the ^{1}H NMR spectrum over a period of several days reveals slow axial ligand exchange, as the resonances of the bound (*R*) enantiomer gradually increase in intensity at the expense of those of the (*S*) enantiomer (Figure S2, Supporting Information). A plot of the enantioselection ratio [*R*]/[*S*] as a function of time shows that the host−guest system reaches thermodynamic equilibrium in 1 to 3 days, depending on the amino alcohol guest (Figure 1). The final equilibrium ratios [*R*]/[*S*] measured by ^{1}H NMR are 1.2, 2.0, and 2.7 (±0.1) for (*R*,*S*)-prolinol, (*R*,*S*)-2-aminobutanol, and (*R*,*S*)-2-aminopropanol, respectively. In each case, the (*R*) enantiomer is the preferentially bound ligand at equilibrium. It is reasonable to assume that the axial Co−N bonds have similar energies in the (*R*) and (*S*) complexes, and thus the preference for (*R*) amino alcohol is the result of stronger noncoordinate binding to the chiroporphyrin host. The time dependence of the enantioselection

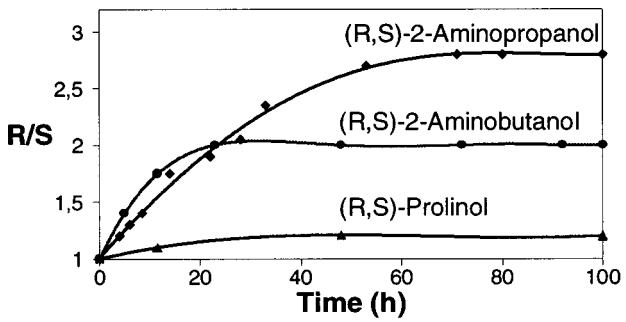

Figure 1. Plot of the enantioselection ratio [*R*]/[*S*] as a function of time for the adducts of **1** with (*R*,*S*)-2-aminopropanol, (*R*,*S*)-2-aminobutanol, and (*R*,*S*)-prolinol. The host−guest system reaches thermodynamic equilibrium in 20 to 80 h, depending on the amino alcohol guest.

(1) Abbreviation: TMCP, dianion of α,*β*,α,*β*-tetramethylchiroporphyrin; EtOH, ethanol.

(2) Mazzanti, M.; Veyrat, M.; Ramasseul, R.; Marchon, J. C.; Turowska-Tyrk, I.; Shang, M.; Scheidt, W. R. *Inorg. Chem.* **1996**, *35*, 3733.

(3) Toronto, D.; Sarrazin, F.; Pécaut, J.; Marchon, J. C.; Shang, M.; Scheidt, W. R. *Inorg. Chem.* **1998**, *37*, 526.

(4) Veyrat, M.; Fantin, L.; Desmoulins, S.; Petitjean, A.; Mazzanti, M.; Ramasseul, R.; Marchon, J. C.; Bau, R. *Bull. Soc. Chim. Fr.* **1997**, *134*, 703.

(5) Enantioselective binding of amino acid derivatives to chiral Zn(II) and Ru(IV) porphyrin complexes has been reported. See, for example: (a) Konishi, K.; Yahara, K.; Toshishige, H.; Aida, T.; Inoue, S. *J. Am. Chem. Soc.* **1994**, *116*, 1337. (b) Mizutani, T.; Ema, T.; Tomita, T.; Kuroda, Y.; Ogoshi, H. *J. Am. Chem. Soc.* **1994**, *116*, 4240. (c) Kuroda, Y.; Kato, Y.; Higashioji, T.; Hasegawa, J.; Kawanami, S.; Takahashi, M.; Shiraishi, N.; Tanabe, K.; Ogoshi, H. *J. Am. Chem. Soc.* **1995**, *117*, 10950. (d) Morice, C.; Le Maux, P.; Simonneaux, G. *Tetrahedron Lett.* **1996**, *37*, 6701. (e) Crossley, M. J.; Mackay, L. G.; Try, A. C. *J. Chem. Soc., Chem. Commun.* **1995**, 1925. See also the following reviews: (f) Pirkle, W. H.; Pochapsky, T. C. *Chem. Rev.* **1989**, *89*, 347. (g) Canary, J. W.; Gibb, B. C. *Progr. Inorg. Chem.* **1997**, *45*, 1.

(6) (a) Parker, D. *Chem. Rev.* **1991**, *91*, 1441. (b) Hulst, R.; Kellogg, R. M.; Feringa, B. L. *Recl. Trav. Chim. Pays-Bas* **1995**, *114*, 115. (c) Staubach, B.; Buddrus, J. *Angew. Chem., Int. Ed. Engl.* **1996**, *35*, 1344. (d) Koy, C.; Michalik, M.; Dobler, C.; Oehme, G. *J. Prakt. Chem.* **1997**, 660.

(7) The observed multiplicities of TMCP *β*-pyrrolic ^{1}H resonances indicate that three distinct complexes are formed: Co(*R*)(*R*), Co(*R*)(*S*), and Co(*S*)(*S*). Each species exhibits two singlets for the *β*-pyrrole protons, characteristic of a D_2 symmetry, presumably due to fast rotation of the axial ligand around the Co−N_{ax} bond. However, the upfield-shifted resonances of the (*R*)− or (*S*)− axial ligands are accidentally isochronous for the "pure" and "mixed" species. See Figure S2 (Supporting Information).

(8) The (*R*)/(*S*) ratios have been obtained by integration of both the upfield-shifted axial ligand resonances and the downfield-shifted *β*-pyrrolic singlet pairs (Figure S2, Supporting Information).

(9) Langford, C. H.; Gray, H. B. *Ligand Substitution Processes*; Benjamin: New York, 1965; pp 55−101.

(10) Martell, A. E.; Smith, R. M. *Critical Stability Constants*; Plenum Press: New York and London, 1975; Vol. 2, pp 1−19.

(11) Crystal data for [**8**$^+$Cl$^-$]·1.5 H_2O·3$CHCl_3$: monoclinic, space group $P2_1$, a = 12.9539(1) Å, b = 22.6358(1) Å, c = 13.4329(2) Å, β = 117.43°, V = 3495.99(6) Å^3, and Z = 2; 15923 reflections were collected and appropriately averaged,[12] 9889 of which were unique (193 K, 1.71° < θ < 26.01°); 9124 reflections [$I > 2\sigma(I)$] yielded R = 0.0446 and R_w = 0.1187. Crystal data for [**9**$^+$Cl$^-$]·4 H_2O·2$CHCl_3$: trigonal, space group $P3_121$, $a = b$ = 20.0467(1) Å, c = 29.9368(5) Å, γ = 120°, V = 10418.9(2) Å^3, and Z = 6; 47456 reflections were collected and appropriately averaged,[12] 12237 of which were unique (193 K, 1.36° < θ < 25.86°); 10483 reflections [$I > 2\sigma(I)$] yielded R = 0.0707 and R_w = 0.1876. Intensity data were collected with a Siemens SMART system.

S0002-7863(98)00644-1 CCC: $15.00
Published on Web 07/11/1998

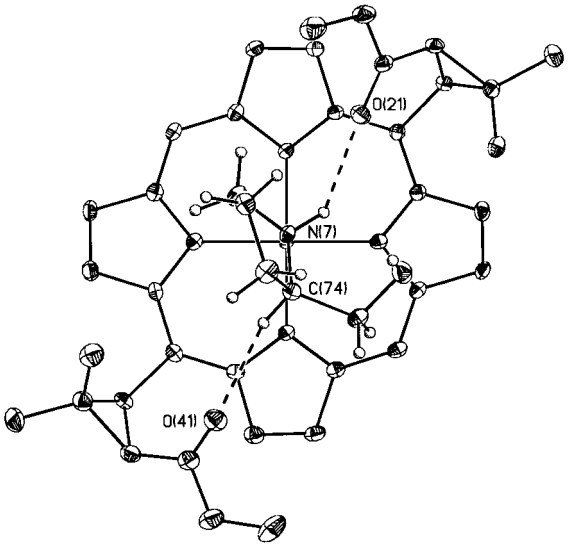

Figure 2. ORTEP view (30% probability) of the X-ray structure of the cobalt(III) chiroporphyrin−bis[(*R*)-prolinol] complex $\mathbf{8}^+$ showing the hydrogen bonding pattern between a (*R*)-prolinol guest and two carbonyl groups of the host on the top face. The other (*R*)-prolinol axial ligand and the two *meso* substituents on the bottom face have been omitted for clarity. The enantiodifferentiating hydrogen bond distances are C(74)···O(41) = 3.230(2) Å (top) and C(64)···O(51) = 3.186(1) Å (bottom, not shown).

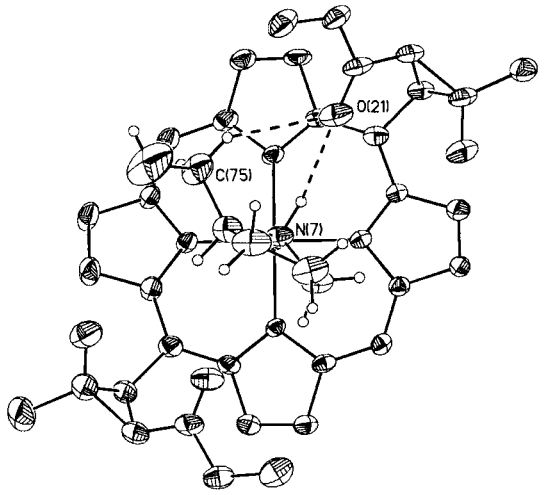

Figure 3. ORTEP view (30% probability) of the X-ray structure of the cobalt(III) chiroporphyrin−bis[(*S*)-prolinol] complex $\mathbf{9}^+$ showing the hydrogen bonding pattern between an (*S*)-prolinol guest and two carbonyl groups of the host on the top face. The other (*S*)-prolinol axial ligand and the two *meso* substituents on the bottom face have been omitted for clarity. The enantiodifferentiating hydrogen bond distances are C(75)···O(21) = 3.400(2) Å (top) and C(65)···O(31) = 3.381(2) Å (bottom, not shown).

ratio suggests that equilibration takes place by a dissociative pathway, and that the rate-determining step is the dissociation of the amino alcohol axial ligand.[9]

The observed difference in dissociation kinetics between cobalt-bound aliphatic amines[3] and amino alcohols is consistent with their known Bronsted basicities. Functionalization of *n*-propylamine ($pK_A = 10.6$) by a hydroxyl group is known to afford a less basic species ($pK_A = 9.6$),[10] which presumably will be a slightly weaker ligand of cobalt(III). The slightly greater dissociation rate constant of the amino alcohol complexes likely will allow slow axial ligand exchange and attainment of the thermodynamic equilibrium, which are not observed for the amine complexes.[3]

The X-ray structures of the (*R*)- and (*S*)-prolinol bis-adducts of Co(III)(TMCP)$^+$, $\mathbf{8}^+Cl^-$ and $\mathbf{9}^+Cl^-$, respectively,[11] show strongly ruffled porphyrin rings (Figures 2 and 3; Figures S7−S10, Supporting Information) and long axial bond distances (average Co−N_{ax}: 2.0517(8) and 2.0458(8) Å, respectively) which result from steric interaction between ligand hydrogen atoms (notably N−H_d and CH_fH_g−OH) and the macrocycle.[12,13] In the two complexes, steric exclusion constrains the prolinol ligands to lie along the chiral grooves which span the porphyrin ring, with similar conformations of the five-membered rings and N−H···O=C hydrogen bonds (N(6)···O(31) = 3.287(1) Å and N(7)···O(21) = 3.273(1) Å for $\mathbf{8}^+$, and N(6)···O(31) = 3.351(2) Å and N(7)···O(21) = 3.341(2) Å for $\mathbf{9}^+$) to a carbonyl group of the host. The opposite absolute configurations of C_2 in the (*R*)- and (*S*)-prolinol ligands result in different patterns of interaction with the *meso* substituents in $\mathbf{8}^+$ and $\mathbf{9}^+$. In the (*S*)-prolinol complex $\mathbf{9}^+$, the methylene of the hydroxymethyl group $C_{1'}$ of each (*S*)-prolinol ligand is involved in a weak C−H···O=C hydrogen bond to a *meso* carbonyl group (C(75)···O(21) = 3.400(2) Å and C(65)···O(31) = 3.381(2) Å). In contrast, it is the asymmetric carbon atom C_2 of each (*R*)-prolinol ligand that is involved in a C−H···O=C hydrogen bond in $\mathbf{8}^+$, and the bonding is a little stronger (C(74)···O(41) = 3.230(2) Å and C(64)···O(51) = 3.186(1) Å, Figures 2 and 3). We believe that the preferential binding of (*R*)-prolinol in solution at equilibrium is the result of this stronger hydrogen bond, since our NMR data[14] indicate that the intramolecular hydrogen bonding patterns are maintained in solution (*vide supra*). A similar comparison between the structures of the two 2-aminopropanol (and two 2-aminobutanol) adducts of **1** is the focus of our current efforts.[15]

In summary, the cobalt(III)(TMCP)−amino alcohol assembly involves a multicomponent bonding pattern between host and guest that integrates at least three crystallographically apparent noncovalent bonds. The dissociation rate of the strong Co−N coordination bond is much slower than those of the two weak hydrogen bonds, and it governs the overall kinetics of enantiomer selection. Weaker C−H···O hydrogen bonding of the (*S*) enantiomer is the probable origin of the thermodynamic preference for the (*R*)-enantiomer. Potential applications in enantiomer recognition, analysis, and separation of β-amino alcohols can be envisioned, particularly for the β-blocking drugs in which enantiomeric purity is critical. This host−guest system may also provide a practical spectroscopic probe for kinetic studies of dissociative processes, in which the chirality of the ligand advantageously replaces isotope labeling.[9]

Acknowledgment. This work was supported by the CEA and the CNRS (Grant No. URA 1194). We thank Françoise Sarrazin, Céline Pérollier, Franck Launay, and René Ramasseul for helpful discussions, Pierre-Alain Bayle for NMR assistance, and Colette Lebrun for obtaining mass spectral data.

Supporting Information Available: ^{1}H NMR spectral data of the adducts of **1** with **2**−**7** and X-ray structural data on $\mathbf{8}^+Cl^-$ and $\mathbf{9}^+Cl^-$ (40 pages, print/PDF). An X-ray crystallographic file, in CIF format, is available through the Internet only. See any current masthead page for ordering information and Web access instructions.

JA980644V

(12) Complete spectroscopic and crystallographic details are provided in the Supporting Information.

(13) For a similar case, see: Scheidt, W. R.; Cunningham, J. A.; Hoard, J. L. *J. Am. Chem. Soc.* **1973**, *95*, 8289.

(14) Selected ^{1}H NMR data ($CDCl_3$, 200 MHz) for $\mathbf{8}^+Cl^-$: δ −5.86 (m, N−H_d), −3.33 (m, C*−H_c), −1.76 (m, CH_fH_g−OH), −0.57 (m, CH_fH_g−OH). Selected ^{1}H NMR data ($CDCl_3$, 200 MHz) for $\mathbf{9}^+Cl^-$: δ −6.00 (m, N−H_d), −3.59 (m, C*−H_c), −1.57 (m, CH_fH_g−OH), −0.61 (m, CH_fH_g−OH). We note that the high anisochronicity of H_f and H_g in both complexes is correlated to their differing locations in the porphyrin ring current, as seen in the crystal structures of $\mathbf{8}^+Cl^-$ and $\mathbf{9}^+Cl^-$. The more shielded H_g sits very close to the porphyrin ring, see Figures 2 and 3.

(15) Subsidiary host−guest interactions which are too weak to be detected in the crystal structures have been ignored. The structures of the (*S*)-aminopropanol and (*S*)-aminobutanol adducts have been solved, and they will be published elsewhere.